Vadose Zone Journal

Cotransport of titanium dioxide nanoparticles and formaldehyde in saturated and unsaturated columns packed with quartz sand

Constantinos V. Chrysikopoulos | **Theodosia V. Fountouli**

School of Chemical and Environmental Engineering, Technical Univ. of Crete, Chania 73100, Greece

Correspondence
Constantinos V. Chrysikopoulos, School of Chemical and Environmental Engineering, Technical Univ. of Crete, 73100 Chania, Greece.
Email: cvc@enveng.tuc.gr

Assigned to Associate Editor Christophe Darnault.

Abstract

Laboratory-scale experiments were conducted to investigate the simultaneous transport of titanium dioxide (TiO_2) nanoparticles and formaldehyde (FA) in columns packed with quartz sand under water saturated and unsaturated flow conditions. The effects of interstitial velocity and solution ionic strength on the TiO_2 and FA cotransport were examined. The experimental results indicated that substantial retention of TiO_2 nanoparticles occurs in both saturated and unsaturated porous media. The solution ionic strength was found to have a noticeable effect on the retention of TiO_2 nanoparticles in the packed columns. Moreover, the results from the TiO_2 nanoparticle transport experiments in water-saturated packed columns suggested that the TiO_2 nanoparticle mass recoveries increased with increasing flow rate. The results from the TiO_2 nanoparticles and FA cotransport experiments in both water saturated and unsaturated packed columns did not reveal a distinct relationship between mass recoveries and flow rate. The transport of FA in both saturated and unsaturated packed columns was hindered in the presence of TiO_2 nanoparticles, especially at high ionic strength. This work provides useful insights into fate and transport of TiO_2 nanoparticles and FA in saturated and unsaturated porous media.

1 | INTRODUCTION

Titanium dioxide (TiO_2) is one of the most commonly used metal oxides in numerous commercial products, including cosmetics, pigments, sunscreens, and pharmaceuticals (Li et al., 2017; Sun et al., 2015; F. Xu, 2018). Titanium dioxide nanoparticles are also used in several environmental remediation applications (Li et al., 2017; Syngouna & Chrysikopoulos, 2017), as well as in agriculture as nanofertilizers and nanopesticides (Baranowska-Wójcik et al., 2020). Extensive use of TiO_2 nanoparticles inevitably leads to their

release into the environment with potential harmful effects to natural ecosystems and to human health (Baranowska-Wójcik et al., 2020).

Titanium dioxide occurs in three different variants: rutile, anatase, and brookite (Sygouni & Chrysikopoulos, 2015). Anatase, in comparison with rutile and brookite, is used more frequently in industrial applications, and it is the most toxic form of TiO_2 (Baranowska-Wójcik et al., 2020). Although TiO_2 is considered as an inert material, prolonged exposure to TiO_2 nanoparticles, even at small doses, can affect vital internal organs and can increase the risk of developing one of many possible serious diseases.

The fate and transport of TiO_2 nanoparticles in porous media has been explored extensively in typical bench-scale laboratory systems (G. Chen et al., 2011, 2012; Fang et al.,

Abbreviations: AWI, air–water interface; DLVO, Derjaguin–Landau–Verwey–Overbeek; FA, formaldehyde; HDD, hydrodynamic diameter; SWI, solid–water interface; UV–Vis, ultraviolet–visible.

2009; Godinez & Darnault, 2011; Han et al., 2014; Sygouni & Chrysikopoulos, 2015; Wang et al., 2014). Most of the published studies examined the effects of ionic strength, pH, temperature, flow rate, moisture content, soil type, and particle concentration under water-saturated flow conditions (G. Chen et al., 2011; Chowdhury et al., 2011; Lv et al., 2016; N. Xu et al., 2018), and fewer studies under water-unsaturated flow conditions (L. Chen et al., 2008, 2010; Fang et al., 2013; Hoggan et al., 2016). Certainly, the air–water interfaces (AWIs) present in unsaturated porous media provide additional degrees of complexity. Adsorption onto the AWIs and film straining can affect the migration and retention of nanoparticles in unsaturated porous media (Hoggan et al., 2016).

Formaldehyde (FA) is a known toxic organic substance that is frequently released in environmental systems because it is used in many different applications (Fountouli et al., 2019; Paliulis, 2016). Therefore, FA removal from wastewater with the use of natural or manufactured sorbents, including engineered carbon nanotubes, is a topic of current research (Georgopoulou & Chrysikopoulos, 2018). Although FA dissolved in wastewaters can eventually infiltrate into the subsurface soil and reach groundwater aquifers, the transport of FA in subsurface formations has not received extensive attention (Fountouli et al., 2019). Fountouli and Chrysikopoulos (2020) investigated the cotransport of two colloid-sized clay particles (kaolinite, KGa-1b, and montmorillonite, STx-1b) with FA in unsaturated porous media and found that the presence of clay particles retarded the transport of FA.

Recent studies revealed that FA adsorbs onto TiO_2 surfaces mainly in a monodentate configuration (Setvin et al., 2017), and FA adsorption onto TiO_2 nanoparticles occurs mainly due to a chemisorption process with pseudo-second-order kinetics (Stefanarou & Chrysikopoulos, 2021). Also, TiO_2 nanoparticles may facilitate the transport of coexisting pollutants and colloidal and biocolloidal particles through porous media (Cai et al., 2013, 2014, 2019; G. Chen et al., 2012; Chowdhury et al., 2012; Fang et al., 2016; Guo et al., 2018; Syngouna et al., 2017; Xia et al., 2019). However, the cotransport of TiO_2 nanoparticles and FA in saturated and unsaturated porous media, to our knowledge, has not been investigated previously. Therefore, this study aimed to explore the cotransport of TiO_2 nanoparticles and FA in bench scale columns packed with quartz sand. The impact of AWIs on the cotransport of TiO_2 nanoparticles and FA in unsaturated porous media was investigated under different flow conditions and different solution ionic strengths.

2 | MATERIALS AND METHODS

2.1 | Formaldehyde

Analytical grade FA (≥99%, Sigma-Aldrich) was used in this study. A master-stock FA solution (1,000 mg L^{-1}) was pre-

Core Ideas

- We study simultaneous transport of titanium dioxide (TiO_2) nanoparticles and formaldehyde (FA).
- The transport of FA in packed columns was hindered in the presence of TiO_2 nanoparticles.
- The solution ionic strength significantly affected TiO_2 retention within the porous medium.

pared using Milli-Q distilled deionized water (ddH_2O) as solvent and stored in a dark bottle at 4 ˚C. All experiments were conducted inside a fume hood with initial FA concentration of $C_0 = 2$ mg L^{-1}, which was prepared by dilution of the master-stock solution. The FA concentration in the various samples collected was determined by the Nash colorimetric method (Nash, 1953), following well-established procedures, using an ultraviolet–visible (UV–Vis) spectrophotometer (Shimadzu, UV-1900), operated at 412 nm (Fountouli et al., 2019; Seyfioglu et al., 2006). The detection limit of this colorimetric technique is 0.17 mM (Economou & Mihalopoulos, 2002).

2.2 | TiO$_2$ nanoparticle suspensions

A master-stock of TiO_2 nanoparticle suspension (1,000 mg L^{-1}) was prepared by mixing TiO_2 powder (anatase < 25 nm in diameter, purity >99.9%, Sigma-Aldrich) with ddH_2O following previously used procedures (Sygouni & Chrysikopoulos, 2015). Particle sizes and zeta potentials were measured in the suspension medium by dynamic light scattering (DLS), using a Zetasizer NanoZS (model ZS90 analyzer, Malvern Instrument). The initial concentration of TiO_2 nanoparticles used in the experiments conducted in this study was 50 mg L^{-1} with pH = 6.8. The TiO_2 concentration of each sample collected was determined by converting the optical densities of the TiO_2 nanoparticles measured at a wavelength of 287 nm (UV-vis spectrophotometer, Shimadzu, UV-1900) to TiO_2 nanoparticle concentrations (Syngouna et al., 2017).

2.3 | Packed columns and transport experiments

The various columns used in this study were packed with quartz sand (Filcom, Sibelco). The sand grain diameter was 0.425–0.600 mm (Sieve no. 30/40). The sand was cleaned thoroughly by following previously established procedures (Lenhart & Saiers, 2002; Syngouna & Chrysikopoulos, 2011).

All saturated and unsaturated column experiments were conducted under three different volumetric flow rates ($Q = 1$, 2 and 3 ml min^{-1}), and two different ionic strengths (0

and 50 mM sodium chloride [NaCl]), at room temperature (~23 ˚C). The saturated experiments were performed in glass columns with length of 30 cm and inner diameter of 2.5 cm, whereas the unsaturated experiments were conducted in Plexiglas columns with length of 15.2 cm and inner diameter of 2.6 cm. For each experiment, fresh, dry quartz sand was used to pack column in small increments under gentle vibration, in order to eliminate the possibility of forming stratified layers (Lewis & Sjostrom, 2010).

All the water-saturated experiments were conducted in vertically oriented packed columns with interstitial flow in the upward direction. Note that the rate of particle deposition is greater for up-flow than down-flow direction (Chrysikopoulos & Syngouna, 2014). The details of the experimental procedures and sample collection were similar to those established in earlier works (Syngouna & Chrysikopoulos, 2011; Chrysikopoulos et al., 2017). The porosity and bulk density of each column were estimated gravimetrically. The various conditions of water saturated experiments are listed in Table 1.

All the unsaturated transport experiments were conducted in vertically oriented packed columns placed on top of a vacuum chamber (Soil Measurement Systems), with flow direction vertically downwards. The details of the experimental procedures and sample collection were similar to those used in earlier studies (Anders & Chrysikopoulos, 2009; Fountouli & Chrysikopoulos, 2020; Mitropoulou et al., 2013). The weight of the initially dry column and the wet column at the end of each experiment were used for the evaluation of the volumetric water content (θ_m) and the degree of saturation (S_w). The three different flow rates used (1, 2, and 3 ml min^{-1}) yielded three different water saturation levels (~40, 50, and 60%, respectively). The various conditions of the unsaturated experiments are listed in Table 1.

3 | THEORETICAL ASPECTS OF MASS RETENTION AND DLVO THEORY

The mass recovered (M_r [–]) of the injected solute and nanoparticles at the effluent of packed columns was determined with the following equation (Chrysikopoulos & Katzourakis, 2015):

$$M_r = \frac{m_0}{M_{in}/U} \qquad (1)$$

where m_0 [T M L^{-3}] is the zeroth moment and represents the total mass in the concentration breakthrough curve (James & Chrysikopoulos, 2011), M_{in} [M L^{-2}] is the mass injected in the column, and U [L T^{-1}] is the interstitial velocity of the fluid.

The classical Derjaguin–Landau–Verwey–Overbeek (DLVO) theory was used to calculate the total interaction

energy, Φ_{DLVO} (h), between TiO$_2$ nanoparticles, as well as the quartz sand, solid–water-interface (SWI), and AWI (Loveland et al. 1996):

$$\Phi_{DLVO}(h) = \Phi_{vdW}(h) + \Phi_{dl}(h) + \Phi_{Born}(h) \qquad (2)$$

where Φ_{vdW} (J), Φ_{dl} (J), and Φ_{Born} (J) are the van der Waals, double layer, and Born potential energies, respectively, and h [L] is the separation distance between the two approaching surfaces. In this study, the TiO$_2$ nanoparticles were considered spheres with diameters equal to their hydrodynamic diameters, and the quartz sand, AWI, and SWI were regarded as infinite plates. Therefore, the various DLVO interaction energies were treated as ideal sphere–plate interactions. For the for sphere–plate model, the Φ_{vdW} interactions were calculated with the expression provided by Gregory (1981), the Φ_{dl} interactions with the expression provided by Hogg et al. (1966), and the Φ_{Born} interactions with the expression provided by Ruckenstein and Prieve (1976). For the Φ_{dl} calculations, it was assumed that the required Stern potentials, Ψ [V], were equal to the corresponding zeta potentials. Furthermore, the required Hamaker constant A_{123} (J) for microscopic bodies of composition "1" and "3" in medium "2" (1 = TiO$_2$, 2 = water, 3 = sand, AWI, or SWI) was determined by the following rule (Israelachvili, 2011):

$$A_{123} = \left(\sqrt{A_{11}} - \sqrt{A_{22}} \right) \left(\sqrt{A_{33}} - \sqrt{A_{22}} \right) \qquad (3)$$

with $A_{11} = 15.3 \times 10^{-20}$ J for TiO$_2$ nanoparticles (Bergström, 1997), $A_{22} = 3.7 \times 10^{-20}$ J for water (Israelachvili, 2011), and $A_{33} = 8.5 \times 10^{-20}$ J for quartz sand (Bergström, 1997). Also, $A_{123} = 1.4 \times 10^{-20}$ J for the system TiO$_2$–water–sand (Wu & Cheng, 2016). Furthermore, based on Equation 3 with $A_{33} = 0$ J for air (Israelachvili, 2011), it was estimated that $A_{123} = -3.5 \times 10^{-20}$ J for the system TiO$_2$–water–air. It should be noted that Hamaker constants with positive value imply that the forces are attractive, whereas Hamaker constants with negative value imply that the forces are repulsive. Often, a DLVO interaction energy profile may contain a primary minimum, Φ_{min1}, a primary maximum, Φ_{max1}, and a secondary minimum, Φ_{min2} (Chrysikopoulos et al., 2012).

4 | RESULTS AND DISCUSSION

The breakthrough TiO$_2$ concentrations collected from the transport experiments in the columns packed with quartz sand, under water-saturated as well as unsaturated conditions, in the absence and presence of salinity (50 mM NaCl) are presented in Figure 1 as a function of pore volume. Three different flow rates (Q = 1, 2, and 3 ml min^{-1}) were considered. The effluent concentrations were

TABLE 1 Experimental conditions and estimated parameter values

Run	TiO$_2$ + FA	NaCl	Q	S_w	U	ρ_b	Θ	HDD	Zeta potential	M_r (TiO$_2$), (FA)
	mg L^{-1}	mM	ml min^{-1}	%	cm min^{-1}	g cm^{-3}		nm	mV	%
Saturated column experiments										
1	50 + 0	0	1	100	0.52	1.73	0.39	138.1	32.3	(24.4), (–)
2	50 + 0	0	2	100	1.02	1.72	0.40	136.1	31.9	(23.3), (–)
3	50 + 0	0	3	100	1.52	1.72	0.40	137.2	26.2	(41.2), (–)
4	50 + 0	50	1	100	0.52	1.74	0.39	2,298	2.6	(0.87), (–)
5	50 + 0	50	2	100	1.00	1.72	0.41	1,871	5.1	(1.76), (–)
6	50 + 0	50	3	100	1.52	1.70	0.40	2,266	7.6	(6.21), (–)
7	50 + 2	0	1	100	0.51	1.70	0.40	136.1	29.0	(13.6), (78.6)
8	50 + 2	0	2	100	1.02	1.71	0.40	133.1	32.0	(49.9), (90.6)
9	50 + 2	0	3	100	1.54	1.70	0.40	136.9	33.0	(41.1), (86.5)
10	50 + 2	50	1	100	0.53	1.75	0.39	2,104	5.9	(1.24), (66.4)
11	50 + 2	50	2	100	1.04	1.74	0.39	1,918	2.4	(0.66), (65.0)
12	50 + 2	50	3	100	1.59	1.75	0.39	1,696	7.5	(1.05),(67.9)
Unsaturated column experiments										
13	50 + 0	0	1	40.9	0.45	1.73	0.39	199.1	18.4	(1.75), (–)
14	50 + 0	0	2	50.1	0.94	1.72	0.40	194.1	13.9	(1.10), (–)
15	50 + 0	0	3	60.0	1.37	1.72	0.40	182.0	14.4	(2.77), (–)
16	50 + 0	50	1	40.1	0.46	1.74	0.39	2,093	13.4	(3.79), (–)
17	50 + 0	50	2	50.4	0.90	1.72	0.41	2,380	12.5	(2.24), (–)
18	50 + 0	50	3	60.1	1.38	1.70	0.40	2,346	12.0	(1.90), (–)
19	50 + 2	0	1	40.2	0.46	1.70	0.40	184.1	20.0	(1.63), (80.3)
20	50 + 2	0	2	50.4	0.90	1.71	0.40	173.4	23.8	(1.27), (78.1)
21	50 + 2	0	3	60.0	1.33	1.70	0.40	208.8	23.9	(9.57), (77.5)
22	50 + 2	50	1	39.5	0.46	1.75	0.39	2,056	2.5	(1.93), (75.2)
23	50 + 2	50	2	50.7	0.91	1.74	0.39	2,089	4.5	(1.62), (67.4)
24	50 + 2	50	3	60.0	1.33	1.75	0.39	2,154	5.3	(1.42), (67.2)

Note. Q, volumetric flow rate; S_w, degree of saturation; U, interstitial velocity; ρ_b, bulk density; θ, porosity; HDD, hydrodynamic diameter; M_r, mass recovery; FA, formaldehyde.

normalized with respect to the initial TiO$_2$ concentration C_0. The experimental conditions as well as the mass recovered (M_r), as estimated with Equation 1, are listed in Table 1. The experimental results suggested that under water-saturated conditions, the TiO$_2$ effluent concentrations and mass recovered progressively increased with increasing flow rate. The positively charged TiO$_2$ nanoparticles were retained by the negatively charged quartz sand, as has also been observed in previous studies (Cai et al., 2013; Chowdhury et al., 2011; Fang et al., 2013; Solovitch et al., 2010; Xia et al., 2019). The M_r of TiO$_2$ nanoparticles was directly proportional to the flow rate. Under unsaturated conditions, the TiO$_2$ effluent concentrations and M_r values were very low for all three flow rates considered in this study. The positively charged TiO$_2$ nanoparticles were almost completely retained by the negatively charged AWIs. Strong interaction between TiO$_2$ nanoparticles and AWIs has also been observed by numer-

ous investigators (L. Chen et al., 2010; Hoggan et al., 2016; Torkzaban et al., 2008; Wan & Tokunaga, 2002). As the water saturation decreased, the AWI areas increased and consequently the retention of TiO$_2$ nanoparticles increased (L. Chen et al., 2010). On the contrary, Fang et al. (2013) reported that AWIs had little effect on the retention and transport of TiO$_2$ nanoparticles in sand columns. For all cases (saturated and unsaturated) shown in Figure 1, the presence of NaCl affected substantially the transport of TiO$_2$ nanoparticles, as suggested by the estimated M_r reduction (see Table 1). The observed increase in TiO$_2$ retention with increasing ionic strength is consistent with the classical DLVO theory due to the compression of the electrical double layer (Lv et al, 2016; Verwey & Overbeek, 1948). Similar observations have been reported by numerous other investigators (G. Chen et al., 2011; Fang et al., 2016; Mukherjee & Weaver, 2010).
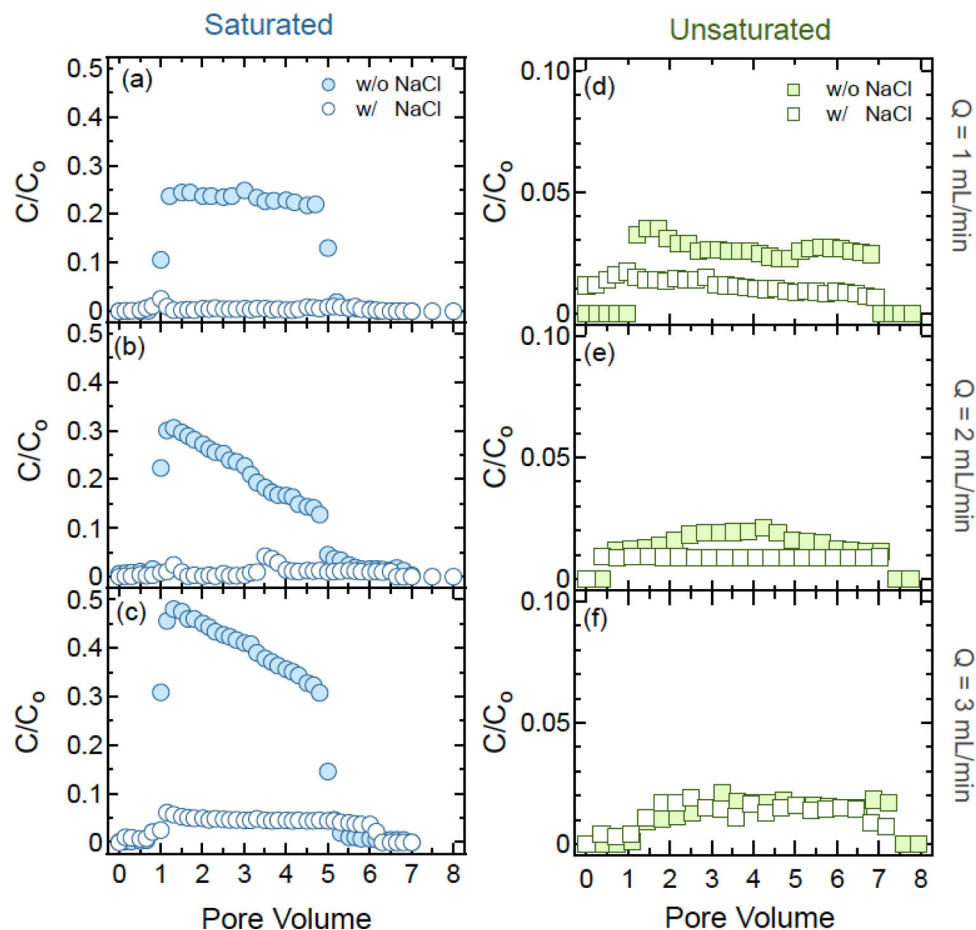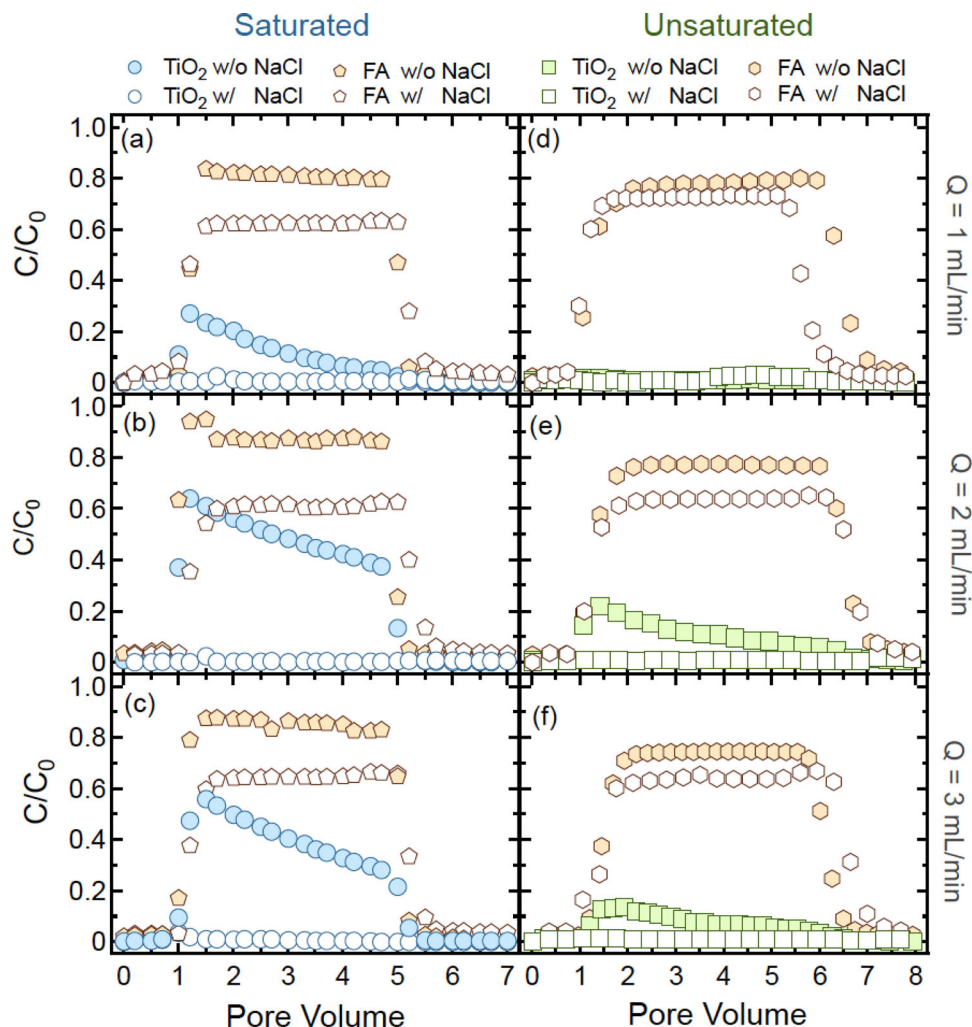
FIGURE 1 Normalized breakthrough curves (C/C_0) of TiO_2 from transport experiments in columns packed with sand, without (filled symbols) and with (open symbols) the presence of NaCl, under (a–c) saturated (a–c, circles) and unsaturated (d–f, squares) conditions, at various flow rates: (a, d) $Q = 1$, (b, e) $Q = 2$, and (c, f) $Q = 3$ ml min^{-1}

The normalized breakthrough concentrations of TiO_2 nanoparticles and FA from the cotransport experiments in columns packed with quartz sand, under water-saturated as well as unsaturated conditions, in the absence and presence of NaCl, for three different flow rates are presented in Figure 2. The experimental conditions are listed in Table 1. For all cases considered here, the presence of NaCl contributed to more pronounced retention of both TiO_2 nanoparticles and FA within the columns. Note that the calculated M_r values were reduced in the presence of NaCl (see Table 1).

Previous studies have shown that the presence of NaCl does not affect FA retention by the quartz sand (Fountouli et al., 2019), and that FA can sorb significantly onto TiO_2 nanoparticles (Stefanarou & Chrysikopoulos, 2021). Furthermore, no significant FA retention by the quartz sand has been observed in batch experiments or in flowthrough experiments in packed columns under both water saturated and unsaturated conditions (Fountouli et al., 2019; Fountouli & Chrysikopoulos, 2020). Consequently, the observed FA retention during cotransport in both saturated and unsaturated columns can be attributed to FA sorption onto TiO_2 nanoparticles, which

subsequently were attached onto quartz sand. As shown by the results from the transport experiments (see Figure 1), the results from the cotransport experiments suggested that the normalized effluent concentration and M_r for the TiO_2 nanoparticles progressively increased with increasing flow rate (see Figure 2 and Table 1), whereas the normalized effluent concentration and M_r of FA remained relatively unaffected by flow rate fluctuations.

The experimental results for the average hydrodynamic diameter (HDD) of a 50-mg L^{-1} TiO_2 suspension, together with the corresponding zeta potential measurements under various conditions are presented in Figure 3. It was shown that the HDD significantly increased from 1,065 to 1,829 nm (see Figure 3a), and the zeta potential decreased from 35.9 to 4.2 mV (see Figure 3b) as the NaCl concentration increased from 30 to 150 mM. The TiO_2 suspensions with NaCl concentrations of <50 mM yielded zeta potential values >30 mV, which are considered to represent stable solutions where nanoparticles are expected to resist aggregation. Consequently, the ionic strength played a significant role on both HDD and zeta potential, due to the electric double layer

FIGURE 2 Normalized breakthrough curves (C/C_0) of TiO_2 and formaldehyde (FA) from cotransport experiments in columns packed with sand, without (filled symbols) and with (open symbols) the presence of NaCl, under (a–c) saturated and (d–f) unsaturated conditions, at various flow rates: (a, d) $Q = 1$, (b, e) $Q = 2$, and (c, f) $Q = 3$ ml min^{-1}

compression. Note that the zeta potential of TiO_2 remained positive, indicating that aggregating particles were positively charged and thus capable of attaching onto negatively charged quartz sand grains. Also, due to their increasing particle size, TiO_2 aggregates could be retained by straining within packed columns. These findings are in agreement with previous studies (Chowdhury et al., 2011; Solovitch et al., 2010; Zhou et al., 2016). It should be noted that the HDD values actually suggest that substantial agglomeration of TiO_2 nanoparticles took place within the packed column during the transport experiments. This observation is in agreement with earlier work on TiO_2 nanoparticles agglomeration in porous media (Sygouni & Chrysikopoulos, 2015), where it was shown that a substantial percentage of the anatase TiO_2 nanoparticles injected into the experimental column were retained within the column packing due to agglomeration.

The effect of pH on HDD and zeta potential of a 50-mg L^{-1} TiO_2 suspension with and without the presence of salin-ity (50 mM NaCl) is also presented in Figure 3. As expected, it was shown that the HDD increased with increasing pH, and HDD values were consistently higher in the presence of NaCl (see Figure 3c). The zeta potential decreased with increasing pH, and the measured zeta potential values were consistently higher in the absence of NaCl, suggesting that the zeta potential was inversely proportional to TiO_2 aggregate size (see Figure 3d). This result is in agreement with previous observations (Sygouni & Chrysikopoulos, 2015). The pH where the electrophoretic mobility switches from positive to negative, known as the isoelectric point (IEP), was found be equal to pH$_{IEP}$ = 6.6 in the absence of NaCl and pH$_{IEP}$ = 5.8 in the presence of 50 mM NaCl. Therefore, the presence of salinity contributes to the formation of larger aggregates with lower zeta potential. It was shown that the TiO_2 aggregate size progressively increased with time, with and without the presence of salinity (50 mM NaCl), in a similar fashion (see Figure 3e). Furthermore, for both cases considered, a slight increase in the
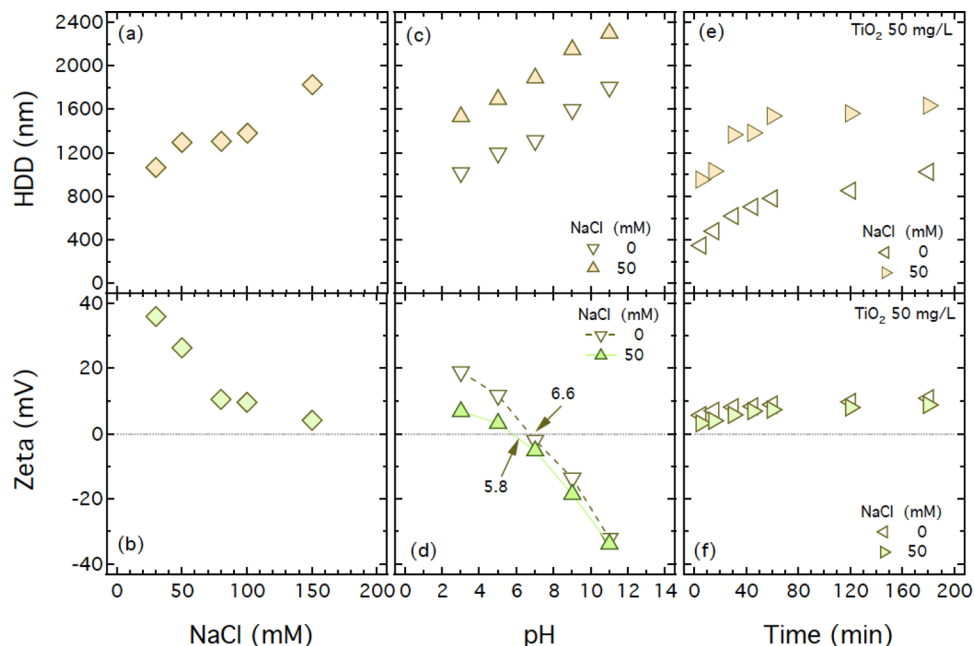
FIGURE 3 Hydrodynamic diameter (HDD) and zeta potential as a function of: (a, b) NaCl concentration, (c, d) pH, and (e, f) time, for a 50-mg L^{-1} TiO_2 solution
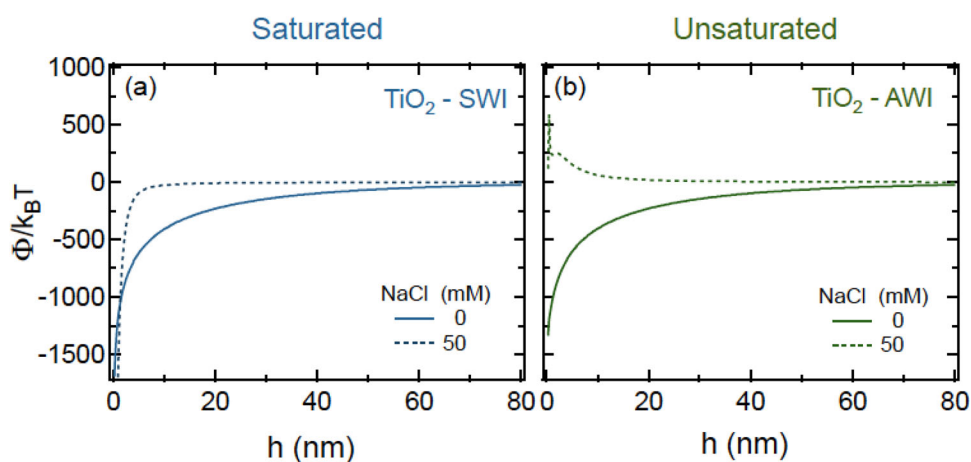
FIGURE 4 Predicted Derjaguin–Landau–Verwey–Overbeek (DLVO) interaction energy (Φ) profiles as a function of separation distance for: (a) TiO_2–SWI (soil–water interface), and (b) TiO_2–AWI (air–water interface), based on the sphere–plate model, without (solid curves) and with (dashed curves) the presence of NaCl. k_B is the Boltzman constant (1.38×10^{-23} J K^{-1}). T is temperature (K). h is the separation distance between the two approaching surfaces

zeta potential was observed with time, as the TiO_2 aggregate size increased (see Figure 3f).

Total Φ_{DLVO} interaction energy profiles for the saturated and unsaturated conditions of this study were determined for the interaction pairs TiO_2 with two different interfaces (AWI and SWI), and they are shown in Figure 4. The estimated interaction energy minima (Φ_{min1} and Φ_{min2}) and energy barrier (Φ_{max1}) values are listed in Table 2. Note that, in the absence of NaCl, the calculated interaction energy profiles for both pairs (TiO_2–SWI and TiO_2–AWI) were very sim-

ilar. Both exhibited a deep primary energy well (less than $-1,000k_BT$, where k_B is the Boltzman constant [1.38×10^{-23} J K^{-1}] and T is temperature [K]), but not an energy barrier. In the presence of NaCl, only the interaction energy profile for the pair TiO_2–AWI exhibited an energy barrier (see Figure 4b). Also, note that the Φ_{min} value decreased with increasing ionic strength (presence of NaCl). An increase in ionic strength results in lower M_r due to energy barrier reduction and in increased tendency for nanoparticle aggregation (Zhang et al., 2015). With the exception of the pair

TABLE 2 Estimated interaction energy barrier (Φ_{max1}) and energy minima (Φ_{min1} and Φ_{min2})

Interacting pair	NaCl	Φ_{max1}	Φ_{min1}	Φ_{min2}
	mM		$k_B T$	
TiO_2–SWI	0	−0.019	−1,691.3	na
TiO_2–SWI	50	−0.046	−5,434.3	na
TiO_2–AWI	0	−0.089	−1,336.4	na
TiO_2–AWI	50	592.2	0.116	na

Note. SWI, soil–water interface; AWI, air–water interface; k_B, Boltzman constant (1.38×10^{-23} J K^{-1}); T, temperature (K); na, not available.

TiO_2–AWI in the presence of NaCl, the other three pairs suggested favorable conditions for TiO_2 attachment onto the quartz sand under the experimental conditions, because the total potential remained negative for long separation distances. These DLVO predictions are consistent with the low M_r observed for TiO_2 under both saturated and unsaturated conditions of this study, which is in agreement with previous work (Xia et al., 2019). Although for the interaction pair TiO_2–AWI in the presence of NaCl, DLVO would predict that particle attachment would be decreased due to the high energy barrier. However, the experimental results of this study have shown the exact opposite trend (see Figure 1, d–f). This contradiction is attributed to the presence of other retention mechanisms (e.g., surface charge heterogeneities, aggregation, straining), which are not accounted by the DLVO theory. Similar contradictions have been reported in several previous studies (Chowdhury et al., 2011; Fang et al., 2013; Solovitch et al., 2010). Furthermore, although secondary energy minima (Φ_{min2}) can play an important role on particles deposition (Zhou et al., 2016), based on the DLVO theory, none of the four interaction pairs considered exhibited Φ_{min2} under the experimental conditions (see Figure 4 and Table. 2).

5 | SUMMARY AND CONCLUSIONS

The experimental results of this study suggested that substantial retention of TiO_2 nanoparticles could occur under both saturated and unsaturated conditions. It was shown that that the majority of TiO_2 nanoparticles were either retained by the quartz sand surfaces or by the gas–water interfaces. The solution ionic strength significantly affected the retention of TiO_2 nanoparticles within the porous medium, an observation that is consistent with zeta potential measurements and the traditional DLVO theory. Higher ionic strengths led to nanoparticle aggregation, which in turn yielded TiO_2 retention in the column. The TiO_2 mass recovered was shown to increase with increasing flow rate in water saturated columns, but no clear trend was observed for the unsaturated columns. The observed FA retention during TiO_2 and FA cotransport experiments in both saturated and unsaturated columns was attributed to FA sorption onto TiO_2 nanoparticles, which subsequently were attached onto quartz sand. Although the DLVO theory predicted a high energy barrier for the interaction pair TiO_2–AWI in the presence of NaCl, the experimental results did not exhibit the anticipated reduction in particle attachment, possibly due to other retention mechanisms that are not accounted by the DLVO theory. The experimental findings of this study suggested that quartz sand can satisfactorily be used to filter TiO_2 nanoparticles from water. Understanding the transport of TiO_2 nanoparticles and FA in porous media is helpful for the prediction of their migration behavior in soil and groundwater systems, thus minimizing their hazardous impacts.

AUTHOR CONTRIBUTIONS
Constantinos V. Chrysikopoulos: Conceptualization; Funding acquisition; Investigation; Project administration; Supervision; Writing-review & editing. Theodosia V. Fountouli: Data curation; Formal analysis; Methodology.

CONFLICT OF INTEREST
The authors declare no conflict of interest.

ORCID
Constantinos V. Chrysikopoulos https://orcid.org/0000-0003-4722-8697

REFERENCES
Anders, R., & Chrysikopoulos, C. V. (2009). Transport of viruses through saturated and unsaturated columns packed with sand. *Transport in Porous Media*, 76, 121–138. https://doi.org/10.1007/s11242-008-9239-3

Baranowska-Wójcik, E., Szwajgier, D., Oleszczuk, P., & Winiarska-Mieczan, A. (2020). Effects of titanium dioxide nanoparticles exposure on human health: A review. *Biological Trace Element Research*, 193, 118–129. https://doi.org/10.1007/s12011-019-01706-6

Bergström, L. (1997). Hamaker constants of inorganic materials. *Advances in Colloid and Interface Science*, 70, 125–169. https://doi.org/10.1016/S0001-8686(97)00003-1

Cai, L., He, L., Peng, S., Li, M., & Tong, M. (2019). Influence of titanium dioxide nanoparticles on the transport and deposition of microplastics in quartz sand. *Environmental Pollution*, 253, 351–357. https://doi.org/10.1016/j.envpol.2019.07.006

Cai, L., Tong, M., Ma, H., & Kim, H. (2013). Cotransport of titanium dioxide and fullerene nanoparticles in saturated porous media. *Environmental Science & Technology*, 47(11), 5703–5710. https://doi.org/10.1021/es400256d

Cai, L., Tong, M., Wang, X., & Kim, H. (2014). Influence of clay particles on the transport and retention of titanium dioxide nanoparticles in quartz sand. *Environmental Science & Technology*, 48, 7323–7332. https://doi.org/10.1021/es5019652

Chen, G., Liu, X., & Su, C. (2011). Transport and retention of TiO_2 rutile nanoparticles in saturated porous media under low-ionic-strength conditions: Measurements and mechanisms. *Langmuir*, 27(9), 5393–5402. https://doi.org/10.1021/la200251v

Chen, G., Liu, X., & Su, C. (2012). Distinct effects of humic acid on transport and retention of TiO_2 rutile nanoparticles in saturated sand columns. *Environmental Science & Technology*, 46(13), 7142–7150. https://doi.org/10.1021/es204010g

Chen, L., Sabatini, D. A., & Kibbey, T. C. G. (2008). Role of the air–water interface in the retention of TiO_2 nanoparticles in porous media during primary drainage. *Environmental Science & Technology*, 42, 1916–1921. https://doi.org/10.1021/es071410r

Chen, L., Sabatini, D. A., & Kibbey, T. C. G. (2010). Retention and release of TiO_2 nanoparticles in unsaturated porous media during dynamic saturation change. *Journal of Contaminant Hydrology*, 118(3–4), 199–207. https://doi.org/10.1016/j.jconhyd.2010.07.010

Chowdhury, I., Cwiertny, D. M., & Walker, S. L. (2012). Combined factors influencing the aggregation and deposition of nano-TiO_2 in the presence of humic acid and bacteria. *Environmental Science & Technology*, 46, 6968–6976. https://doi.org/10.1021/es2034747

Chowdhury, I., Hong, Y., Honda, R. J., & Walker, S. L. (2011). Mechanisms of TiO_2 nanoparticle transport in porous media: Role of solution chemistry, nanoparticle concentration, and flowrate. *Journal of Colloid and Interface Science*, 360(2), 548–55. https://doi.org/10.1016/j.jcis.2011.04.111

Chrysikopoulos, C. V., & Katzourakis, V. E. (2015). Colloid particle size-dependent dispersivity. *Water Resources Research*, 51, 4668–4683. https://doi.org/10.1002/2014WR016094

Chrysikopoulos, C. V., Sotirelis, N. P., & Kallithrakas-Kontos, N. G. (2017). Cotransport of graphene oxide nanoparticles and kaolinite colloids in porous media. *Transport in Porous Media*, 119, 181–202. https://doi.org/10.1007/s11242-017-0879-z

Chrysikopoulos, C. V., & Syngouna, V. I. (2014). Effect of gravity on colloid transport through water-saturated columns packed with glass beads: Modeling and experiments. *Environmental Science & Technology*, 48, 6805–6813. https://doi.org/10.1021/es501295n

Chrysikopoulos, C. V., Syngouna, V. I., Vasiliadou, I. A., & Katzourakis, V. E. (2012). Transport of *Pseudomonas putida* in a three-dimensional bench scale experimental aquifer. *Transport in Porous Media*, 94, 617–642. https://doi.org/10.1007/s11242-012-0015-z

Economou, C., & Mihalopoulos, N. (2002). Formaldehyde in the rainwater in the eastern Mediterranean: Occurrence, deposition and contribution to organic carbon budget. *Atmospheric Environment*, 36, 1337–1347. https://doi.org/10.1016/S1352-2310(01)00555-6

Fang, J., Shan, X.-Q., Wen, B., Lin, J.-M., & Owens, G. (2009). Stability of titania nanoparticles in soil suspensions and transport in saturated homogeneous soil columns. *Environmental Pollution*, 157(4), 1101–1109. https://doi.org/10.1016/j.envpol.2008.11.006

Fang, J., Xu, M.-J., Wang, D.-J., Wen, B., & Han, J.-Y. (2013). Modeling the transport of TiO_2 nanoparticle aggregates in saturated and unsaturated granular media: Effects of ionic strength and pH. *Water Research*, 47, 1399–1408. https://doi.org/10.1016/j.watres.2012.12.005

Fang, J., Zhang, K., Sun, P., Lin, D., Shen, B., & Luo, Y. (2016). Cotransport of $Pb^{(2+)}$ and TiO_2 nanoparticles in repacked homogeneous soil columns under saturation condition: Effect of ionic strength and fulvic acid. *The Science of the Total Environment*, 571, 471–478. https://doi.org/10.1016/j.scitotenv.2016.07.013

Fountouli, T. V., & Chrysikopoulos, C. V. (2020). Effect of clay colloid particles on formaldehyde transport in unsaturated porous media. *Water*, 12, 3541. https://doi.org/10.3390/w12123541

Fountouli, T. V., Chrysikopoulos, C. V., & Tsanis, I. K. (2019). Effect of salinity on formaldehyde interaction with quartz sand and kaolinite colloid particles: Batch and column experiments. *Environmental Earth Sciences*, 78, 152. https://doi.org/10.1007/s12665-019-8147-x

Georgopoulou, M. P., & Chrysikopoulos, C. V. (2018). Evaluation of carbon nanotubes and quartz sand for the removal of formaldehyde–(2,4-dinitrophenylhydrazine) from aqueous solutions. *Industrial & Engineering Chemistry Research*, 57(49), 17003–17012.

Gregory, J. (1981). Approximate expressions for retarded van der Waals interaction. *Journal of Colloid and Interface Science*, 83(1), 138–145. https://doi.org/10.1016/0021-9797(81)90018-7

Godinez, I. G., & Darnault, C. J. G. (2011). Aggregation and transport of nano-TiO_2 in saturated porous media: Effects of pH, surfactants and flow velocity. *Water Research*, 45, 839–851. https://doi.org/10.1016/j.watres.2010.09.013

Guo, P., Xu, N., Li, D., Huangfu, X., & Li, Z. (2018). Aggregation and transport of rutile titanium dioxide nanoparticles with montmorillonite and diatomite in the presence of phosphate in porous sand. *Chemosphere*, 204, 327–334. https://doi.org/10.1016/j.chemosphere.2018.04.041

Han, P., Wang, X., Cai, L., Tong, M., & Kim, H. (2014). Transport and retention behaviors of titanium dioxide nanoparticles in iron oxide-coated quartz sand: Effects of pH, ionic strength, and humic acid. *Colloids and Surfaces, A: Physicochemical and Engineering Aspects*, 454, 119–127. https://doi.org/10.1016/j.colsurfa.2014.04.020

Hogg, R., Healy, T. W., & Fuerstenau, D. W. (1966). Mutual coagulation of colloidal dispersions. *Transactions of the Faraday Society*, 62, 1638–1651. https://doi.org/10.1039/tf9666201638

Hoggan, J. L., Sabatini, D. A., & Kibbey, T. C. G. (2016). Transport and retention of TiO_2 and polystyrene nanoparticles during drainage from tall heterogeneous layered columns. *Journal of Contaminant Hydrology*, 194, 30–35. https://doi.org/10.1016/j.jconhyd.2016.10.003

Israelachvili, J. N. (2011). *Intermolecular and surface forces* (3rd ed.) Academic Press.

James, S. C., & Chrysikopoulos, C. V. (2011). Monodisperse and polydisperse colloid transport in water-saturated fractures with various orientations: Gravity effects. *Advances in Water Resources*, 34, 1249–1255. https://doi.org/10.1016/j.advwatres.2011.06.001

Lenhart, J. J., & Saiers, J. E. (2002). Transport of silica colloids through unsaturated porous media: Experimental results and model comparisons. *Environmental Science & Technology*, 36(4), 769–777. https://doi.org/10.1021/es0109949

Lewis, J., & Sjöstrom, J. (2010). Optimizing the experimental design of soil columns in saturated and unsaturated transport experiments. *Journal of Contaminant Hydrology*, 115, 1–13. https://doi.org/10.1016/j.jconhyd.2010.04.001

Li, X., Yoneda, M., Shimada, Y., & Matsui, Y. (2017). Effect of surfactants on the aggregation and stability of TiO_2 nanomaterial in environmental aqueous matrices. *The Science of the Total Environment*, 574, 176–182. https://doi.org/10.1016/j.scitotenv.2016.09.065

Loveland, J. P., Ryan, J. N., Amy, G. L., & Harvey, R. W. (1996). The reversibility of virus attachment to mineral surfaces. *Colloids and*

Surfaces A, *107*, 205–221. https://doi.org/10.1016/0927-7757(95)03373-4

Lv, X., Tao, J., Chen, B., & Zhu, X. (2016). Roles of temperature and flow velocity on the mobility of nano-sized titanium dioxide in natural waters. *The Science of the Total Environment*, *565*, 849–856. https://doi.org/10.1016/j.scitotenv.2016.03.001

Mitropoulou, P. N., Syngouna, V. I., & Chrysikopoulos, C. V. (2013). Transport of colloids in unsaturated packed columns: Role of ionic strength and sand grain size. *Chemical Engineering Journal*, *232*, 237–248. https://doi.org/10.1016/j.cej.2013.07.093

Mukherjee, B., & Weaver, J. W. (2010). Aggregation and charge behavior of metallic and nonmetallic nanoparticles in the presence of competing similarly-charged inorganic ions. *Environmental Science & Technology*, *44*, 3332–3338. https://doi.org/10.1021/es903456e

Nash, T. (1953). The colorimetric estimation of formaldehyde by means of the Hantzsch reaction. *Biochemical Journal*, *55*, 416–421. https://doi.org/10.1042/bj0550416

Paliulis, D. (2016). Removal of formaldehyde from synthetic wastewater using natural and modified zeolites. *Polish Journal of Environmental Studies*, *25*(1), 251—257. https://doi.org/10.15244/pjoes/60727

Ruckenstein, E., & Prieve, D. C. (1976). Adsorption and desorption of particles and their chromatographic separation. *Aiche Journal*, *22*, 276–283. https://doi.org/10.1002/aic.690220209

Setvin, M., Hulva, J., Wang, H., Simschitz, T., Schmid, M., Parkinson, G. S., Di Valentin, C., Selloni, A., & Diebold, U. (2017). Formaldehyde adsorption on the anatase Tio2(101) surface: Experimental and theoretical investigation. *The Journal of Physical Chemistry C*, *121*, 8914–8922. https://doi.org/10.1021/acs.jpcc.7b01434

Seyfioglu, R., Odabasi, M., & Cetin, E. (2006). Wet and dry deposition of formaldehyde in Izmir, Turkey. *Science of the Total Environment*, *366*, 809–818. https://doi.org/10.1016/j.scitotenv.2005.08.005

Solovitch, N., Labille, J., Rose, J., Chaurand, P., Borschneck, D., Wiesner, M. R., & Bottero, J.-Y. (2010). Concurrent aggregation and deposition of TiO₂ nanoparticles in a sandy porous media. *Environmental Science & Technology*, *44*(13), 4897–4902. https://doi.org/10.1021/es1000819

Stefanarou, A. S., & Chrysikopoulos, C. V. (2021). Interaction of titanium dioxide with formaldehyde in the presence of quartz sand under static and dynamic conditions. *Water*, *13*, 1420. https://doi.org/10.3390/w13101420

Sun, P., Zhang, K., Fang, J., Lin, D., Wang, M., & Han, J. (2015). Transport of TiO₂ nanoparticles in soil in the presence of surfactants. *Science of the Total Environment*, *527–528*, 420–428. https://doi.org/10.1016/j.scitotenv.2015.05.031

Sygouni, V., & Chrysikopoulos, C. V., (2015). Characterization of TiO₂ nanoparticle suspensions in aqueous solutions and TiO₂ nanoparticle retention in water saturated columns packed with glass beads. *Chem. Eng. J.*, *262*, 823–830. https://doi.org/10.1016/j.cej.2014.10.044

Syngouna, V. I., & Chrysikopoulos, C. V., (2011). Transport of biocolloids in water saturated columns packed with sand: Effect of grain size and pore water velocity. *Journal of Contaminant Hydrology*, *126*, 301–314. https://doi.org/10.1016/j.jconhyd.2011.09.007

Syngouna, V. I., & Chrysikopoulos, C. V., (2017). Inactivation of MS2 bacteriophage by titanium dioxide nanoparticles in the presence of quartz sand with and without ambient light. *Journal of Colloid and Interface Science*, *497*, 117–125. https://doi.org/10.1016/j.jcis.2017.02.059

Syngouna, V. I., Chrysikopoulos, C. V., Kokkinos, P., Tselepi, M. A., & Vantarakis, A., (2017). Cotransport of human adenoviruses with clay colloids and TiO₂ nanoparticles in saturated porous media: Effect of flow velocity. *Science of the Total Environment*, *598*, 160–167. https://doi.org/10.1016/j.scitotenv.2017.04.082

Torkzaban, S., Bradford, S. A., van Genuchten, M. Th., & Walker, S. L. (2008). Colloid transport in unsaturated porous media: The role of water content and ionic strength on particle straining. *Journal of Contaminant Hydrology*, *96*(1–4),113–127. https://doi.org/10.1016/j.jconhyd.2007.10.006

Verwey, E. J. W., & Overbeek, J. T. G. (1948). *Theory of the stability of lyophobic colloids: The interaction of soil particles having an electric double layer*. Elsevier.

Wan, J., & Tokunaga, T. K. (2002). Partitioning of clay colloids at air–water interfaces. *Journal of Colloid and Interface Science*, *247*, 54–61. https://doi.org/10.1006/jcis.2001.8132

Wang, X., Cai, L., Han, P., Lin, D., Kim, H., & Tong, M. (2014). Cotransport of multi-walled carbon nanotubes and titanium dioxide nanoparticles in saturated porous media. *Environmental Pollution*, *195*, 31–38. https://doi.org/10.1016/j.envpol.2014.08.011

Wu, Y., & Cheng, T. (2016). Stability of nTiO₂ particles and their attachment to sand: Effects of humic acid at different pH. *The Science of the Total Environment*, *541*, 579–589. https://doi.org/10.1016/j.scitotenv.2015.09.116

Xia, T., Lin, Y., Guo, X., Li, S., Cui, J., Ping, H., Zhang, J., Zhong, R., Du, L., Han, C., & Zhu, L. (2019). Co-transport of graphene oxide and titanium dioxide nanoparticles in saturated quartz sand: Influences of solution pH and metal ions. *Environmental Pollution*, *251*, 723–730. https://doi.org/10.1016/j.envpol.2019.05.035

Xu, F. (2018). Review of analytical studies on TiO₂ nanoparticles and particle aggregation, coagulation, flocculation, sedimentation, stabilization. *Chemosphere*, *212*, 662–677. https://doi.org/10.1016/j.chemosphere.2018.08.108

Xu, N., Cheng, X., Zhou, K., Xu, X., Li, Z., Chen, J., Wang, D., & Li, D. (2018). Facilitated transport of titanium dioxide nanoparticles via hydrochars in the presence of ammonium in saturated sands: Effects of pH, ionic strength, and ionic composition. *The Science of the Total Environment*, *612*, 1348–1357. https://doi.org/10.1016/j.scitotenv.2017.09.023

Zhang, R., Zhang, H., Tu, C., Hu, X., Li, L., Luo, Y., & Christie, P. (2015). Facilitated transport of titanium dioxide nanoparticles by humic substances in saturated porous media under acidic conditions. *Journal of Nanoparticle Research*, *17*, 165. https://doi.org/10.1007/s11051-015-2972-y

Zhou, D. D., Jiang, X. H., Lu, Y., Fan, W., Huo, M. X., & Crittenden, J. C. (2016). Cotransport of graphene oxide and Cu (II) through saturated porous media. *The Science of the Total Environment*, *550*, 717–726. https://doi.org/10.1016/j.scitotenv.2016.01.141